






Induced Pluripotent Stem Cells From Subjects With Primary Sclerosing Cholangitis Develop a Senescence Phenotype Following Biliary Differentiation

Nidhi Jalan-Sakrikar ^{1,2}, Thiago M. De Assuncao,^{1,2} Amaia Navarro-Corcuera,^{1,2} Feda H. Hamdan,^{1,2} Lorena Loarca,^{1,3} Lindsey A. Kirkeby,⁴ Zachary T. Resch,⁴ Steven P. O'Hara,^{1,3,5} Brian D. Juran,^{1,3} Konstantinos N. Lazaridis ^{1,3,5}, Charles B. Rosen,⁶ Julie K. Heimbach,⁶ Timucin Taner ⁶, Vijay H. Shah ^{1,2,5,6}, Nicholas F. LaRusso,^{1,3,5,6} and Robert C. Huebert ^{1,2,5,6}

Primary sclerosing cholangitis (PSC) is a chronic fibroinflammatory disease of the biliary tract characterized by cellular senescence and periportal fibrogenesis. Specific disease features that are cell intrinsic and either genetically or epigenetically mediated remain unclear due in part to a lack of appropriate, patient-specific, *in vitro* models. Recently, our group developed systems to create induced pluripotent stem cell (iPSC)-derived cholangiocytes (iDCs) and biliary epithelial organoids (cholangioids). We use these models to investigate whether PSC cholangiocytes are intrinsically predisposed to cellular senescence. Skin fibroblasts from healthy controls and subjects with PSC were reprogrammed to pluripotency, differentiated to cholangiocytes, and subsequently grown in three-dimensional matrigel-based culture to induce formation of cholangioids. RNA sequencing (RNA-seq) on iDCs showed significant differences in gene expression patterns, including enrichment of pathways associated with cell cycle, senescence, and hepatic fibrosis, that correlate with PSC. These pathways also overlapped with RNA-seq analysis on isolated cholangiocytes from subjects with PSC. Exome sequencing on the subjects with PSC revealed genetic variants of unknown significance in the genes identified in these pathways. Three-dimensional culture revealed smaller size, lack of a central lumen, and increased cellular senescence in PSC-derived cholangioids. Congruent with this, PSC-derived iDCs showed increased secretion of the extracellular matrix molecule fibronectin as well as the inflammatory cytokines interleukin-6, and chemokine (C-C motif) ligand 2. Conditioned media (CM) from PSC-derived iDCs more potently activated hepatic stellate cells compared to control CM. **Conclusion:** We demonstrated efficient generation of iDCs and cholangioids from patients with PSC that show disease-specific features. PSC cholangiocytes are intrinsically predisposed to cellular senescence. These features are unmasked following biliary differentiation of pluripotent stem cells and have functional consequences in epithelial organoids. (*Hepatology Communications* 2022;6:345-360).

P rimary sclerosing cholangitis (PSC) is a complex cholangiopathy for which no universally effective medical therapy exists. The disease is characterized by idiopathic fibro-obliterative destruction of the large and small bile ducts that ultimately leads to strictures, cholestasis, progressive periportal

Abbreviations: 2/3D, two/three dimensional; α -SMA, alpha-smooth muscle actin; β -gal, β -galactosidase; CCL2, C-C motif chemokine ligand 2; CK, cytokeratin; CM, conditioned media; DE, definitive endoderm; EV, extracellular vesicle; FN, fibronectin; GSEA, gene set enrichment analysis; HP, hepatic progenitor; HS, hepatic specification; HSC, hepatic stellate cell; iDC, induced pluripotent stem cell-derived cholangiocyte; IL, interleukin; IPA, ingenuity pathway analysis; iPSC, induced pluripotent stem cell; Nanog, Nanog homeobox; OCT4, POU class 5 homeobox 1; PSC, primary sclerosing cholangitis; RGD, arginylglycylaspartic acid; RNA-seq, RNA sequencing; RT-PCR, reverse-transcription polymerase chain reaction; SASP, senescence-associated secretory phenotype; Sox, SRY-box transcription factor; SSEA, stage-specific embryonic antigen 3.

Received January 14, 2021; accepted July 26, 2021.

Additional Supporting Information may be found at onlinelibrary.wiley.com/doi/10.1002/hep4.1809/supinfo.

fibrogenesis, and a predisposition to cholangiocarcinoma. The phenotype of PSC ranges from benign intrahepatic strictures that rarely progress to severe and rapidly progressive disease that leads to early liver transplantation. The pathophysiology of the disease is complex and multifactorial, involving a complex intersection of genetics, epigenetics, environmental exposures in susceptible individuals, as well as interactions with the microbiome and the immune system.⁽¹⁾ We hypothesized that certain features of PSC, such as cellular senescence, are intrinsic to cholangiocytes, genetically/epigenetically encoded, and may emerge following biliary differentiation. Because of this complexity, standard cell culture and animal models are inadequate to test these hypotheses. Individualized disease models, such as those used in this study, could provide additional insight into certain aspects of disease pathogenesis and allow for targeted therapies to emerge. In particular, the induced pluripotent stem cell (iPSC)-based approach can help to define aspects of PSC that are intrinsic to cholangiocytes and that may be genetically or epigenetically mediated, while the three-dimensional (3D) organoid-based culture system can identify functionally relevant consequences.

The phenomenon of cholangiocyte senescence is increasingly implicated in the pathobiology of PSC.⁽²⁻⁴⁾ During cellular senescence, normal cholangiocytes undergo replication arrest yet remain metabolically active. Senescent cells can be identified by their expression of certain characteristic marker proteins, such as beta-galactosidase (β -gal). Senescent cells also typically display the senescence-associated secretory phenotype (SASP), which includes massive release of inflammatory cytokines, fibrogenic growth factors, and extracellular vesicles (EVs) that promote hepatic stellate cell (HSC) activation and disease progression.⁽²⁾ However, the underlying causes of cholangiocyte senescence in PSC remain obscure. Therefore, we sought to determine whether PSC cholangiocytes are intrinsically predisposed to cellular senescence and whether epithelial organoids derived from them are phenotypically and functionally distinct from controls.

We have an established and well-characterized methodology to generate individualized cholangiocytes from patients with liver disease by using iPSCs.⁽⁵⁾ In this method, skin fibroblasts are isolated and cultured from patients and reprogrammed to pluripotency using standard reprogramming factors. We then

Supported by American Association for the Study of Liver Diseases Foundation Pilot Research Award (AASLD #15 to N.J.S.), National Institutes of Health, National Institute of Diabetes and Digestive and Kidney Diseases (awards DK118619 to K.N.L., DK057993 and DK084567 to N.F.L., DK059615 to V.H.S., and DK100575, DK113339, and DK117861 to R.C.H.), Satter Foundation (N.J.S), and Mayo Clinic Center for Regenerative Medicine.

The content is solely the responsibility of the authors and does not necessarily represent the official views of the National Institutes of Health.

© 2021 The Authors. Hepatology Communications published by Wiley Periodicals LLC on behalf of American Association for the Study of Liver Diseases. This is an open access article under the terms of the Creative Commons Attribution-NonCommercial-NoDerivs License, which permits use and distribution in any medium, provided the original work is properly cited, the use is non-commercial and no modifications or adaptations are made.

View this article online at wileyonlinelibrary.com.

DOI 10.1002/hep4.1809

Potential conflict of interest: Nothing to report.

ARTICLE INFORMATION:

From the ¹Division of Gastroenterology and Hepatology, Mayo Clinic and Foundation, Rochester, MN, USA; ²Gastroenterology Research Unit, Mayo Clinic and Foundation, Rochester, MN, USA; ³Center for Basic Research in Digestive Diseases, Mayo Clinic and Foundation, Rochester, MN, USA; ⁴Center for Regenerative Medicine, Mayo Clinic and Foundation, Rochester, MN, USA; ⁵Center for Cell Signaling in Gastroenterology, Mayo Clinic and Foundation, Rochester, MN, USA; ⁶William J. von Liebig Center for Transplantation and Clinical Regeneration, Mayo Clinic and Foundation, Rochester, MN, USA.

ADDRESS CORRESPONDENCE AND REPRINT REQUESTS TO:

Robert C. Huebert, M.D.
Gastroenterology Research Unit, Mayo Clinic
200 First Street SW

Rochester, MN 55905, USA
E-mail: huebert.robert@mayo.edu
Tel.: +1-507-284-1006

pursue a stepwise differentiation strategy toward cholangiocytes by using biliary morphogens to mimic bile duct development. In this study, for the first time, we generated iPSC-derived cholangiocytes (iDCs) from subjects with PSC undergoing liver transplantation and from healthy living liver donors. These patient-derived cholangiocytes were then used for individualized disease modeling with genome-wide sequencing and organoid-based approaches. We used these novel methods to test whether PSC-derived iDCs efficiently differentiate toward cholangiocytes and whether they can recapitulate certain features seen in PSC, such as altered gene expression patterns, cellular senescence, SASP, and ability to activate HSCs.

Materials and Methods

SKIN FIBROBLAST FROM CONTROLS AND PATIENTS WITH PSC

Under an institutional-approved protocol, subjects with liver disease were identified from the Hepatobiliary Clinic, the Cholestasis Clinic, the Liver Transplant Clinic, or the Liver Transplant Hospital Service at Mayo Clinic, Rochester, MN. Informed consent in writing was obtained from each patient. Healthy controls were selected from a pool of living liver donors who had undergone an extensive predonation evaluation to ensure no occult liver disease was present. Following informed consent, subjects and controls underwent a clinic-based skin biopsy in the Regenerative Medicine Consult Clinic or an operative skin biopsy at the time of liver transplantation or living liver donation. Skin fibroblasts were isolated, expanded, cataloged, and cryopreserved in the Center for Regenerative Medicine Biotrust Laboratory (Mayo Clinic).

CELLULAR REPROGRAMMING

Selected normal and PSC fibroblast samples were reprogrammed to pluripotency at Regen Theranostics by forced expression of Kruppel-like factor 4 (KLF4); POU class 5 homeobox 1 (OCT4); SRY-box transcription factor 2 (SOX2); and MYC proto-oncogene, bHLH transcription factor (c-MYC). Three separate iPSC clones were generated from each patient. iPSC clones underwent extensive quality control, including differentiation to all three primary germ

layers (endoderm, mesoderm, and ectoderm), karyotype analysis, and both staining and flow cytometry for pluripotency markers (Oct4, stage-specific embryonic antigen 3 [SSEA], Nanog homeobox (Nanog), and T-cell receptor alpha locus [TRA-1-60]). A single clone from each patient was then selected for differentiation to cholangiocytes.

STELLATE CELL ACTIVATION ASSAYS

On the last day of differentiation, iDCs were washed with phosphate-buffered saline and replaced with basal media for 24 hours. This conditioned media (CM) was used to treat primary human HSCs (ScienCell #5300) at early passages (P1-P4) overnight.⁽⁶⁾ HSCs were then fixed and stained for alpha-smooth muscle actin (α -SMA; Abcam #ab5694) and collagen (Southern Biotech #1310-01). Dimethyl sulfoxide or 200 nM arginylglycylaspartic acid (RGD) peptide was added to the CM before HSC treatment; 24 hours later, HSCs were collected and analyzed by reverse-transcription polymerase chain reaction (RT-PCR).

STATISTICAL ANALYSIS

Data represent typical experiments reproduced at least 3 times. Data were analyzed by analysis of variance with Bonferroni posttest or paired *t* test, using GraphPad Prism software (GraphPad Software, Inc., La Jolla, CA). The difference was considered significant at $P < 0.05$. Results are presented as mean \pm SEM (refer to Supporting Information for other methods and detailed information).

Results

SAMPLES FROM PATIENTS WITH PSC CAN BE REPROGRAMMED NORMALLY TO iPSC CLONES

We suspected that PSC-derived fibroblasts would reprogram normally to iPSCs. To test this, we first reprogrammed fibroblasts from 3 healthy controls (living liver donors) and 4 subjects with PSC (who underwent liver transplantation) to pluripotency using the standard Yamanaka reprogramming factors (Table 1). In addition to classical stem cell morphology with tightly packed colonies and high nuclear-to-cytoplasmic ratio,

TABLE 1. LISTS OF FIBROBLASTS FROM PATIENTS WITH VARIOUS LIVER DISEASES AS AN EFFORT TO BUILD A LIVER BIOBANK

BioTrust ID	Age	Sex	Diagnosis	Sample Obtained (Date)	Sample Obtained	BioTrust Storage	iPS Clones
014-BIOTR-0001*	49	M	Primary sclerosing cholangitis	9/9/2014	Skin Biopsy	Fibroblasts	4
014-BIOTR-0002	46	M	Carol's disease	10/20/2014	Skin Biopsy	Fibroblasts	
014-BIOTR-0003	62	F	Polycystic liver disease	11/7/2014	Skin Biopsy	Fibroblasts	4
014-BIOTR-0004	32	F	Low phospholipid-associated cholelithiasis	12/18/2014	Skin Biopsy	Fibroblasts	
014-BIOTR-0005	42	M	Primary sclerosing cholangitis	12/22/2014	Skin Biopsy	Fibroblasts	
014-BIOTR-0006	75	F	Primary sclerosing cholangitis	1/19/2015	Skin Biopsy	Fibroblasts	
014-BIOTR-0007	72	F	Primary biliary cirrhosis	1/21/2015	Skin Biopsy	Fibroblasts	3
014-BIOTR-0008	32	M	Cystic fibrosis	2/3/2015	Skin Biopsy	Fibroblasts	
014-BIOTR-0009	59	F	Primary biliary cirrhosis	2/3/2015	Skin Biopsy	Fibroblasts	
014-BIOTR-0010*	46	M	Primary sclerosing cholangitis	2/24/2015	Skin Biopsy	Fibroblasts	4
014-BIOTR-0011	63	F	Polycystic liver disease	2/24/2015	Skin Biopsy	Fibroblasts	
014-BIOTR-0012	35	F	Progressive familial intrahepatic cholestasis, type III	3/13/2015	Skin Biopsy	Fibroblasts	
014-BIOTR-0014	35	M	Cirrhosis	4/14/2015	Skin Biopsy	Fibroblasts	
014-BIOTR-0015	38	M	Healthy donor	4/15/2015	Surgical Skin	Fibroblasts	
014-BIOTR-0016	40	F	Primary sclerosing cholangitis/ cholangiocarcinoma	4/15/2015	Surgical Skin	Fibroblasts	
014-BIOTR-0017	36	M	Primary sclerosing cholangitis/ cholangiocarcinoma	4/17/2015	Surgical Skin	Fibroblasts	
014-BIOTR-0018	38	F	Healthy donor	4/17/2015	Surgical Skin	Fibroblasts	
014-BIOTR-0019	35	F	Polycystic liver disease	4/22/2015	Skin Biopsy	Fibroblasts	
014-BIOTR-0020	33	M	Healthy donor	4/29/2015	Surgical Skin	Fibroblasts	
014-BIOTR-0021	35	M	Idiopathic ductopenia/liver tx	4/29/2015	Surgical Skin	Fibroblasts	
014-BIOTR-0022	33	F	Healthy donor	5/8/2015	Surgical Skin	Fibroblasts	
014-BIOTR-0023	61	F	Primary biliary cirrhosis/liver tx	5/8/2015	Surgical Skin	Fibroblasts	
014-BIOTR-0024	53	M	Cholestatic liver disease/liver tx	5/11/2015	Surgical Skin	Fibroblasts	
014-BIOTR-0025	51	F	Healthy donor	5/11/2015	Surgical Skin	Fibroblasts	
014-BIOTR-0026	52	F	Healthy donor	6/9/2015	Surgical Skin	Fibroblasts	
014-BIOTR-0027	32	M	Alcoholic cirrhosis/liver tx	6/9/2015	Surgical Skin	Fibroblasts	
014-BIOTR-0028*	39	F	Healthy donor	6/15/2015	Surgical Skin	Fibroblasts	4
014-BIOTR-0030*	35	M	Healthy donor	7/6/2015	Surgical Skin	Fibroblasts	4
014-BIOTR-0032	30	F	Erythropoietic protoporphyria/liver tx	7/9/2015	Skin Biopsy	Fibroblasts	
014-BIOTR-0033	25	M	Healthy donor	7/14/2015	Surgical Skin	Fibroblasts	
014-BIOTR-0034	59	M	Hepatic venous outflow obstruction/liver tx	7/14/2015	Surgical Skin	Fibroblasts	
014-BIOTR-0035*	32	M	Primary sclerosing cholangitis/liver tx	8/5/2015	Surgical Skin	Fibroblasts	4
014-BIOTR-0036*	29	M	Healthy donor	8/5/2015	Surgical Skin	Fibroblasts	4

TABLE 1. Continued

BioTrust ID	Age	Sex	Diagnosis	Sample Obtained (Date)	Sample Obtained	BioTrust Storage	iPS Clones
014-BIOTR-0037	30	M	Ornithine transcarbamylase deficiency	9/21/2015	Skin Biopsy	Fibroblasts	
014-BIOTR-0038	45	F	Primary biliary cirrhosis/liver tx	10/9/2015	Surgical Skin	Fibroblasts	
014-BIOTR-0039	54	F	Primary biliary cirrhosis/liver tx	11/16/2015	Surgical Skin	Fibroblasts	
014-BIOTR-0042	30	M	Primary sclerosing cholangitis/liver tx	2/19/2016	Surgical Skin	Fibroblasts	
014-BIOTR-0043	25	M	Primary sclerosing cholangitis	2/23/2016	Skin Biopsy	Fibroblasts	
014-BIOTR-0044	30	F	Primary sclerosing cholangitis	2/24/2016	Skin Biopsy	Fibroblasts	
014-BIOTR-0045	30	M	Primary sclerosing cholangitis/liver tx	6/21/2016	Surgical Skin	Fibroblasts	
014-BIOTR-0046	68	F	Nonalcoholic steatohepatitis/liver tx	7/18/2016	Surgical Skin	Fibroblasts	
014-BIOTR-0048	57	F	Primary sclerosing cholangitis; liver tx	8/2/2016	Skin Biopsy	Fibroblasts	
014-BIOTR-0049	40	F	Primary biliary cirrhosis	8/2/2016	Skin Biopsy	Fibroblasts	
014-BIOTR-0051	43	F	Polycystic Liver disease/liver tx	9/23/2016	Surgical Skin	Fibroblasts	
014-BIOTR-0052	58	F	Primary sclerosing cholangitis/liver tx/ cholangiocarcinoma	1/25/2017	Skin Biopsy	Fibroblasts	
014-BIOTR-0053	36	F	Primary sclerosing cholangitis/liver tx	1/26/2017	Skin Biopsy	Fibroblasts	
014-BIOTR-0054*	29	F	Primary sclerosing cholangitis/liver tx	1/30/2017	Skin Biopsy	Fibroblasts	4
014-BIOTR-0055	55	M	Primary sclerosing cholangitis	3/8/2017	Skin Biopsy	Fibroblasts	
014-BIOTR-0057	65	M	Primary sclerosing cholangitis/liver tx	3/29/2017	Skin Biopsy	Fibroblasts	
014-BIOTR-0058	54	F	Primary sclerosing cholangitis	3/29/2017	Skin Biopsy	Fibroblasts	
014-BIOTR-0059	52	M	Primary sclerosing cholangitis/liver tx	3/30/2017	Skin Biopsy	Fibroblasts	
014-BIOTR-0060	67	M	Primary sclerosing cholangitis/liver tx	4/17/2017	Skin Biopsy	Fibroblasts	
014-BIOTR-0061	58	M	Primary sclerosing cholangitis/liver tx	4/18/2017	Skin Biopsy	Fibroblasts	
014-BIOTR-0062	64	M	Primary sclerosing cholangitis	4/25/2017	Skin Biopsy	Fibroblasts	
014-BIOTR-0065	25	M	Cholestatic liver disease	8/8/2017	Skin Biopsy	Fibroblasts	
014-BIOTR-0066	31	M	Cholestatic liver disease	8/9/2017	Skin Biopsy	Growing	
014-BIOTR-0067	28	F	Primary sclerosing cholangitis	9/6/2017	Skin Biopsy	Growing	
014-BIOTR-0068	54	F	Primary sclerosing cholangitis	9/21/2017	Skin Biopsy	Fibroblasts	
014-BIOTR-0069	41	M	Hepatocellular carcinoma secondary to chronic hepatitis B	9/26/2018	Skin Biopsy	Fibroblasts	
014-BIOTR-0070	69	F	Primary sclerosing cholangitis	6/26/2019	Skin Biopsy	Fibroblasts	
014-BIOTR-0071	65	F	Polycystic liver disease, autosomal dominant	2/4/2020	Skin Biopsy	Fibroblasts	

*Patients used for the present study.
Abbreviations: F, female; M, male; tx, transplant.

the presence of pluripotency markers was confirmed using immunostaining for Oct4 and SSEA and flow cytometry analysis for Oct4, SSEA, Nanog, and Tra-1-60 (Fig. 1A,B; Supporting Figs. S1-S6). Karyotype analysis was performed on all clones, and only clones with normal karyotype were used for further studies (Fig. 1C; Supporting Figs. S1-S6). iPSC clones were evaluated for their ability to differentiate into all three primary germ layers. Following ectoderm, endoderm, or mesoderm differentiation, cells stained positive for neuroepithelial stem cell protein (Nestin) and paired box protein Pax-6 (Pax-6) (ectoderm markers), forkhead box A2 (FoxA2) and SRY-box transcription

factor 17 (Sox17) (endoderm markers), or neural cell adhesion molecule (NCAM) and brachyury (mesoderm markers), respectively, indicating efficient tri-lineage differentiation (Fig. 1D; Supporting Figs. S1-S6).

iPSCs FROM PATIENTS WITH PSC DIFFERENTIATE INTO CHOLANGIOCYTES AS EFFICIENTLY AS CONTROLS

We hypothesized that iPSCs derived from patients with PSC would differentiate efficiently to

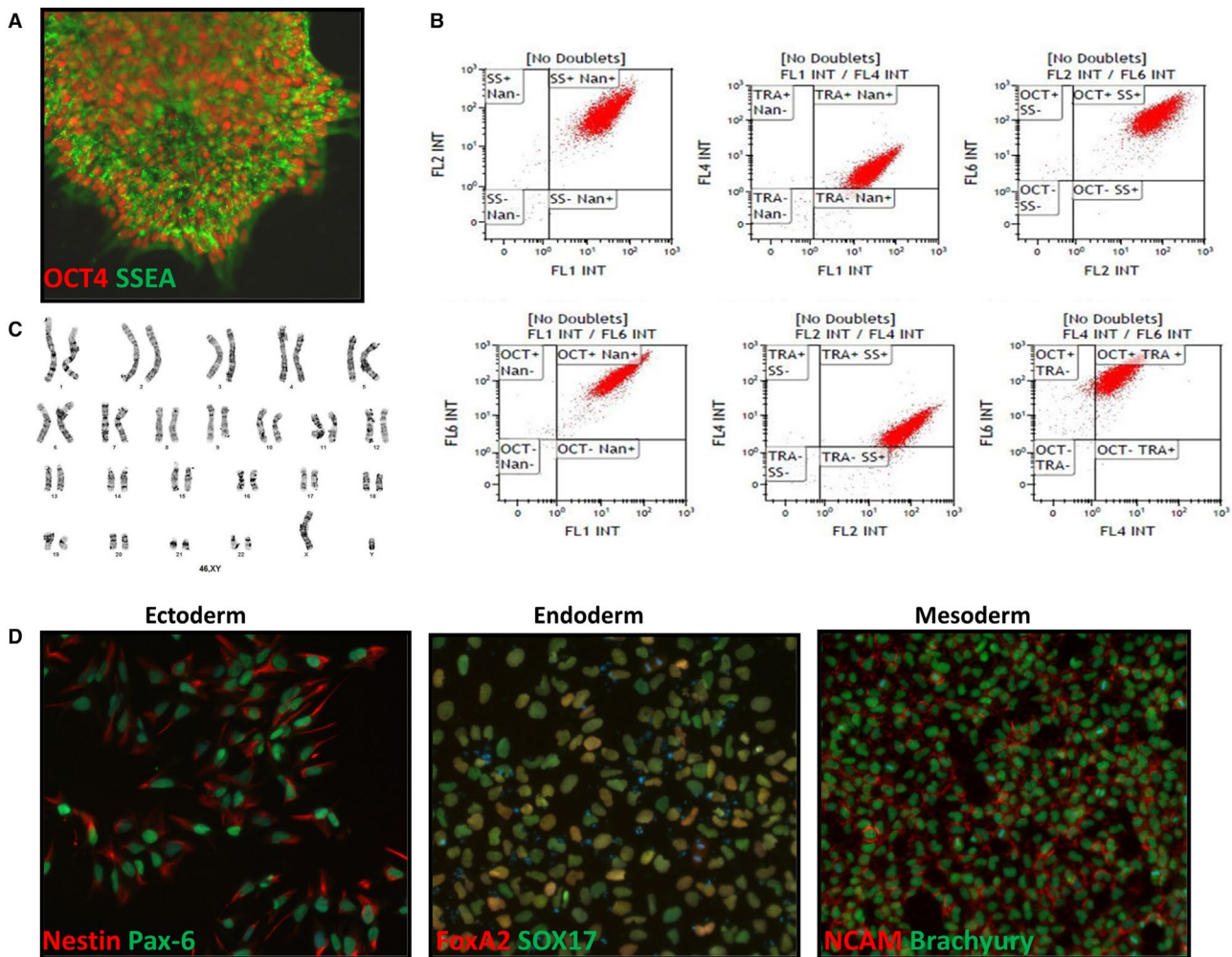


FIG. 1. Quality control analysis on the iPSC clones. (A) iPSC clone stained for pluripotency marker OCT4 (red) and SSEA (green). (B) Flow cytometry analysis for the pluripotency markers on the iPSC clone show greater than 96% purity for the clone. (C) Karyotype analysis shows no abnormalities in the clone. (D) Immunostaining for the three germ layer markers (Nestin and Pax-6 for ectoderm, FoxA2 and SOX17 for endoderm, NCAM and brachyury for mesoderm) shows the ability of the iPSCs to differentiate. Abbreviations: FL INT, Fluorescence Intensity; FoxA2, forkhead box A2; Nan, Nanog; NCAM, neural cell adhesion molecule; Nestin, neuroepithelial stem cell protein; OCT4, POU class 5 homeobox 1; Pax-6, paired box protein Pax-6; SS, Somatostatin; TRA, T-cell receptor alpha locus.

cholangiocytes. Using our published protocol, we differentiated the iPSCs from both the healthy controls and patients with PSC toward cholangiocytes.⁽⁵⁾ Both control and PSC samples demonstrated loss of stem cell morphology and acquired an epithelial cell phenotype following differentiation (Fig. 2A; representative images shown from control and PSC patient 3). Based on the acquisition of cholangiocyte markers cytokeratin 17 (CK-7) and CK-19, we noted efficient differentiation of the iPSCs derived from both healthy controls and subjects with PSC. Both RT-PCR (Fig. 2B) and western blotting (Fig. 2C) demonstrated progressive acquisition of the biliary cyto

keratins as the cells progressed through the five phases of differentiation (iPSC, definitive endoderm [DE], hepatic specification [HS], hepatic progenitor [HP], iDC). We then evaluated for the presence of primary cilia by western blot (Supporting Fig. S7A) and immunofluorescence staining (Fig. 2D) for acetylated α -tubulin in our normal and PSC-derived iDCs. Western blotting for other cilia markers, i.e., adenosine diphosphate ribosylation factor-like guanosine triphosphatase 3 (ARL3) and intraflagellar transport 88 (IFT88) (Supporting Fig. S7A), further confirmed the presence of primary cilia in the iDCs, and we found no significant differences between the normal and PSC-derived cells. We also verified nuclear

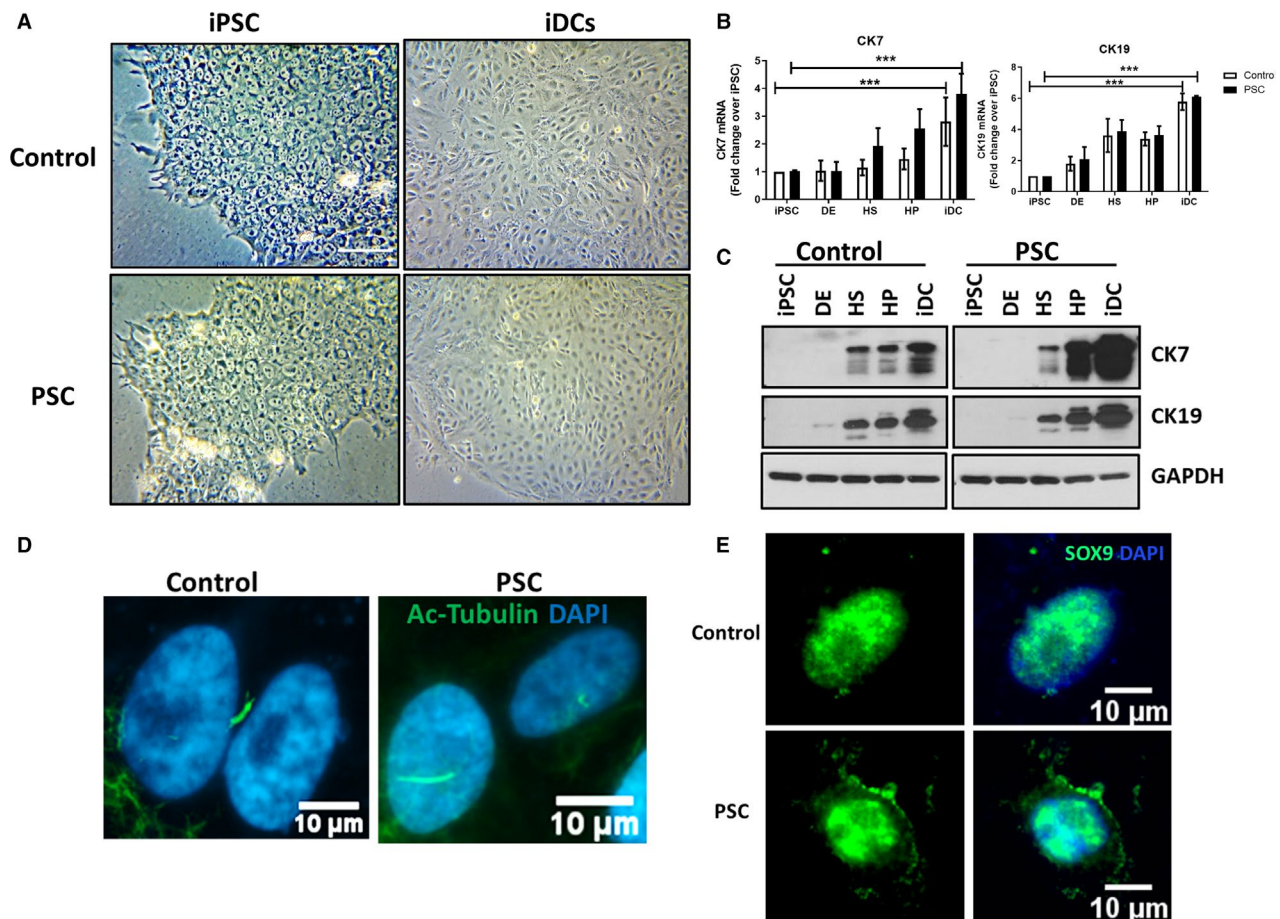


FIG. 2. Differentiation of iPSCs from healthy controls and patients with PSC. (A) Differential interference contrast images of iPSCs and differentiated iPSCs to iDCs from a healthy control and patient with PSC. Scale bar = 50 μ m (B) RT-PCR analysis on iPSC-iDC differentiation showing progressive acquisition of biliary markers CK7 and CK19 for both the healthy control and PSC patient 3. (C) Western blot for CK7 and CK19 of the iPSC to iDC differentiation for both healthy control and PSC patient 3; Data represented as Mean \pm SEM *** P < 0.0001. (D) Immunofluorescence on iDCs showing the presence of cilia (green for acetylated tubulin and blue for DAPI) on the iDCs obtained from both the healthy patient and PSC patient 3. (E) SOX9 (green) immunostaining on iDCs from a healthy control and PSC patient 3. Abbreviations: Ac, acetylated; DAPI, 4',6-diamidino-2-phenylindole; GAPDH, glyceraldehyde 3-phosphate dehydrogenase; mRNA, messenger RNA.

staining of the cholangiocyte transcription factor SOX9 (Fig. 2E) as well as expression of biliary transporters (cystic fibrosis transmembrane conductance regulator [CFTR], apical sodium–bile acid transporter [ASBT]), anion-exchanger 2 [AE2], G-protein-coupled bile acid receptor 1 [TGR5], and the transcription factor hepatocyte nuclear factor 1 beta [HNF1 β] (Supporting Fig. S7A,B). Functionally, we confirmed that the cells have intact secretin-induced cyclic adenosine monophosphate signaling (Supporting Fig. S7C). Overall, these data confirm that iPSCs derived from subjects with PSC differentiate as efficiently as those derived from healthy controls. We have previously demonstrated that these CK7-positive and CK19-positive cells also express other cholangiocyte markers, such as aquaporin 1 (AQP-1), have intact adenosine triphosphate-induced calcium signaling, and can engraft in mouse liver following retrograde intrabiliary infusion.⁽⁵⁾

RNA SEQUENCING DEMONSTRATES ENRICHMENT OF THE SENEESCENCE PATHWAY IN PSC-DERIVED iDCs

We anticipated that certain pathological gene expression patterns would be recapitulated in iDCs derived from patients with PSC. To investigate whether known features of PSC can be recapitulated in the differentiated cholangiocytes, we performed transcriptomic analysis in three biological replicates of control (3 living donors) and PSC- (4 patients) derived iDCs using RNA sequencing (RNA-seq). Heat-map analysis ($P < 0.05$, and log-fold change > 2) showed many genes up-regulated in PSC samples (Fig. 3A). The analysis identified 1,261 genes that are significantly differentially expressed between PSC-derived iDCs and the control group ($P < 0.05$). Notably, gene set enrichment analysis (GSEA) identified several pathways enriched in PSC-derived iDCs that are known to be dysregulated in PSC, including anaphase-promoting complex (APC) targets, enhancer of zeste 2 polycomb repressive complex 2 subunit [EZH2] targets, interleukin-6 (IL)-6 signaling, and the senescence pathway (Fig. 3B; Supporting Fig. S7B). Ingenuity pathway analysis (IPA) of the differentially expressed genes further confirmed the senescence features of the PSC-derived iDCs as well as a proinflammatory and fibrogenic profile (Fig. 3C). This is in agreement with Enrichr analysis that

showed an enrichment of cell-cycle pathway in our PSC-derived iDCs (Fig. 3D). Furthermore, transcription factor analysis revealed tumor protein P53 (p53), E2F transcription factor 1 (E2F1), ATM serine/threonine kinase (ATM), and myc pathways enriched in our gene set from PSC-derived iDCs (Fig. 3D). Additional analysis showed that 79% of the genes altered in PSC-derived iDCs were associated with the cell cycle and 21% were involved in senescence (Fig. 3E). Thus, the transcriptomic analysis of the iDCs from patients with PSC suggests that indeed the cholangiocytes derived from skin fibroblasts of patients express some of the pathological gene expression profiles that characterize the disease.

GENE PROFILE OF PSC-DERIVED iDCs OVERLAPS WITH OTHER PSC DATA SETS

In order to further validate the disease relevance of our gene expression observations, we compared the genes up-regulated in our data set to publically available genomic data on PSC. The gene expression profile found in PSC-derived iDCs includes several genes that have been reported to be associated with PSC, including major histocompatibility complex class II, DQ beta 1 (*HLA-DQB1*); histone deacetylase 7 (*HDAC7*); SET domain containing 1A, histone lysine methyltransferase (*SETD1*); and several others⁽⁷⁾ (Fig. 4A). Furthermore, Enrichr analysis on these genes identified sclerosing cholangitis as the top disease followed by other autoimmune diseases (Fig. 4B). To gain additional insight into our iPSC-derived iDCs, we performed GSEA with a custom data set that included up-regulated genes in cholangiocytes isolated from patients with PSC compared to healthy controls.⁽³⁾ Interestingly we observed significant enrichment of these genes in our PSC-derived iDCs, further supporting their recapitulation of gene expression profiles found in cholangiocytes from patients with PSC (Fig. 4C). Particularly, 78 genes were found in both data sets (Fig. 4D) that are mostly associated with epithelial to mesenchymal transition and inflammatory processes (Fig. 4E). Additionally, IPA showed that 134 of 142 pathways were corepresented in both the iDCs and the human PSC samples (Fig. 4F; Supporting Table S2). Overall, these data demonstrate that the iDCs recapitulate many gene expression changes seen in patients with PSC.

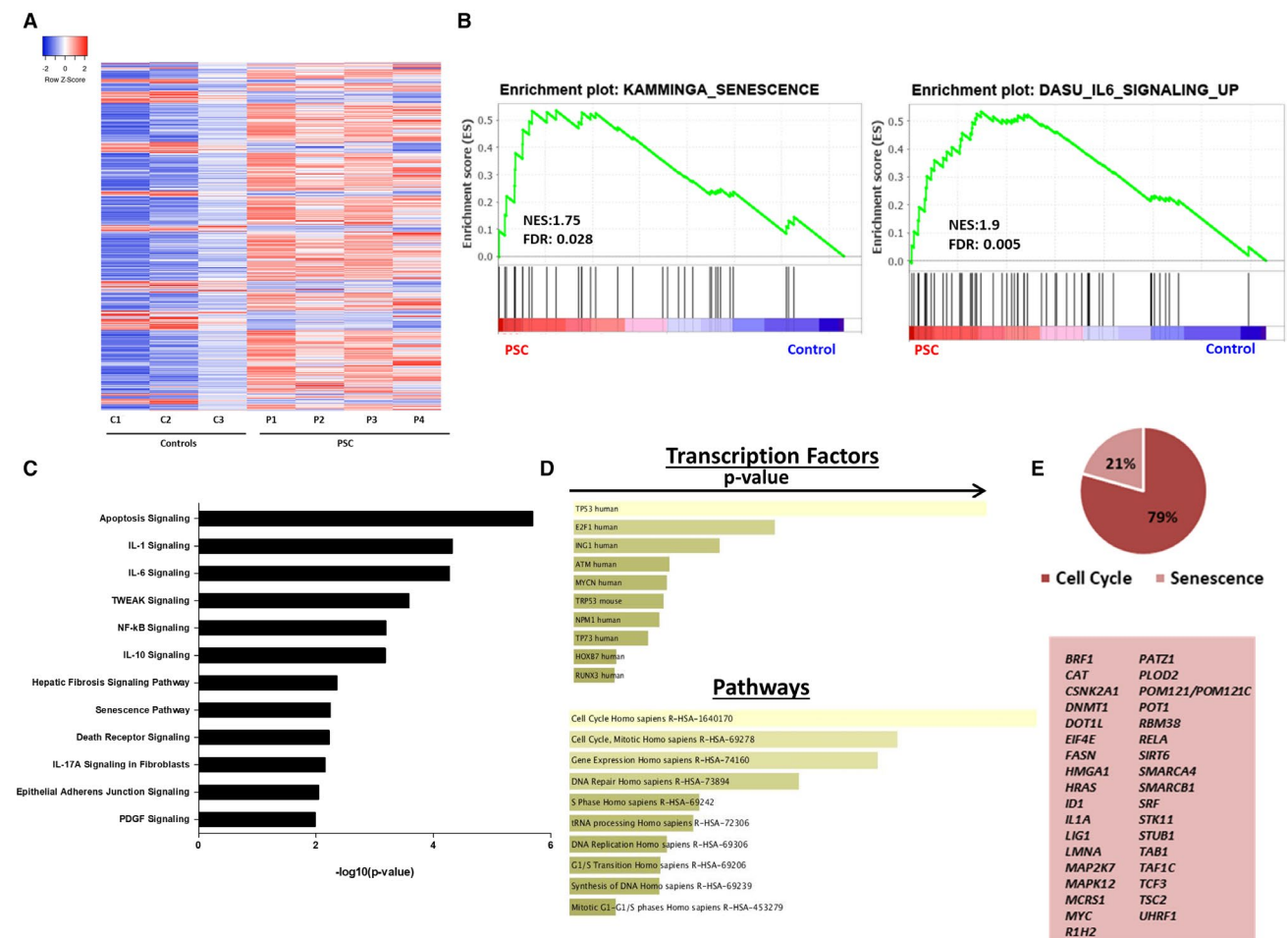


FIG. 3. RNA-seq analysis on the iDCs. (A) Heat map showing gene expression analysis for all the healthy and PSC clones used in the study; red shows up regulated, blue shows down regulated. (B) GSEA analysis revealing pathways enriched in our gene set. (C) Canonical pathways associated with differentially expressed genes in iPSC-derived iDCs show senescence, hepatic fibrosis, and inflammatory pathways. (D) Enrichr analysis on the up-regulated genes in PSC samples show transcription factors and pathways implicated in cell cycle and senescence. (E) Pie chart generated from IPA reveals 21% of the altered genes in PSC-derived iDCs are involved in senescence; the lower panel shows some of the senescence genes. Abbreviations: ATM, ataxia telangiectasia mutated; BRF1, BRF1 RNA Polymerase III Transcription Initiation Factor Subunit; CAT, Chloramphenicol acetyltransferase; CSNK2A1, Casein Kinase 2 Alpha 1; DNMT1, DNA Methyltransferase 1; DOT1L, Disruptor of telomeric silencing 1-like; E2F1, E2F Transcription Factor 1; EIF4E, Eukaryotic Translation Initiation Factor 4E; FASN, Fatty Acid Synthase; FDR, false discovery rate; HMG1, High Mobility Group AT-Hook 1; HOXB7, Homeobox B7; HRAS, HRas Proto-Oncogene; ID1, Inhibitor Of DNA Binding 1; IL1A, Interleukin 1A; ING, inhibitor of growth; LIG1, DNA Ligase 1; LMNA, Lamin A/C; MAP2K7, Mitogen-Activated Protein Kinase Kinase 7; MAPK12, Microspherule Protein 1; Mitogen-Activated Protein Kinase 12; MYC, MYC Proto-Oncogene; MYCN, MYCN Proto-Oncogene, BHLH Transcription Factor; NES, normalized enrichment score; NFKB, nuclear factor-kappa B; NPM1, Nucleophosmin; PATZ1, POZ/BTB And AT Hook Containing Zinc Finger 1; PLOD2, Procollagen-Lysine, 2-Oxoglutarate 5-Dioxygenase 2; POM121, POM121 Transmembrane Nucleoporin; POT1, Protection of Telomeres 1; R1H2, rox1-helix2; RBM38, RNA-binding motif protein 38; RELA, RELA Proto-Oncogene, NF-KB Subunit; RUNX3, RUNX Family Transcription Factor 3; SIRT6, Sirtuin 6; SMARCA4, SWI/SNF Related, Matrix Associated, Actin Dependent Regulator Of Chromatin, Subfamily A, Member 4; SMARCB1, SWI/SNF Related, Matrix Associated, Actin Dependent Regulator Of Chromatin, Subfamily B; SRF, Serum Response Factor; STK11, Serine-Threonine Kinase 11; STUB1, STIP1 homology and U-Box containing protein 1; TAB1, TGF-Beta Activated Kinase 1; TAF1C, TATA-Box Binding Protein Associated Factor, RNA Polymerase I Subunit C; TCF3, Transcription Factor 3; TP53, Tumor Protein 53; TP73, Tumor Protein P73; TRP53, transformation-related protein 53; TSC2, Tuberous Sclerosis Complex 2; TWEAK, TNF-related weak inducer of apoptosis; UHRF1, Ubiquitin Like With PHD And Ring Finger Domains 1

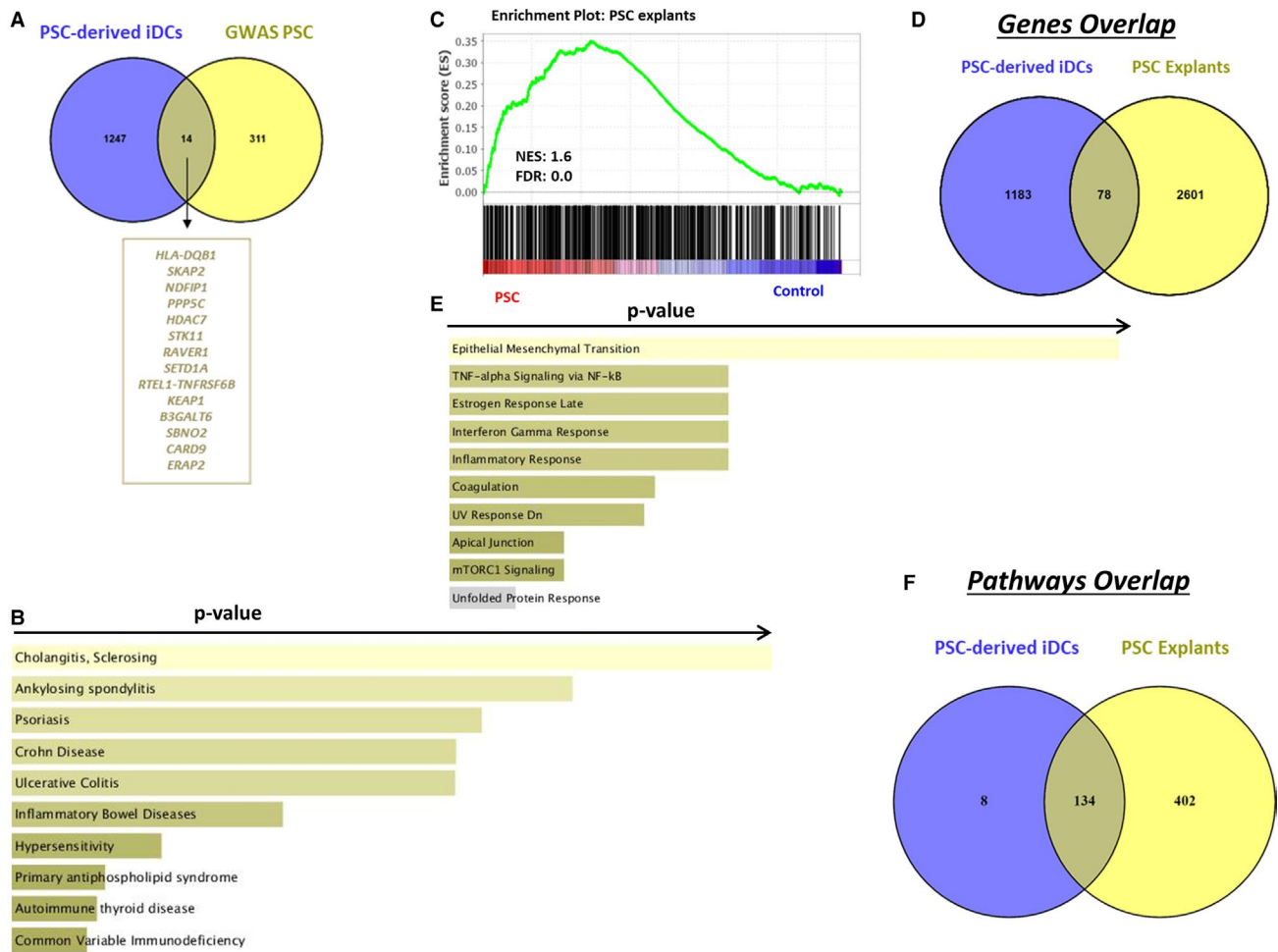


FIG. 4. Comparison of PSC-derived iDCs with PSC gene profile data sets. (A) Venn diagram depicting 14 genes that are common in PSC-derived iDCs with the GWASs on patients with PSC. (B) Enrichr analysis on the common 14 genes showing sclerosing cholangitis as the top disease being represented. (C) GSEA analysis on iDC RNA-seq compared to the up-regulated genes in cholangiocytes from patients with PSC. (D) Venn diagram depicting 78 genes common between the PSC-derived iDCs and PSC explants. (E) Enrichr analysis on the common 78 genes showing epithelial–mesenchymal transition, inflammatory responses as top pathways. (F) Venn diagram depicting 134 pathways common between the PSC-derived iDCs and PSC explants. Abbreviations: B3GALT6, Beta-1,3-Galactosyltransferase 6; CARD9, Caspase Recruitment Domain Family Member 9; ERAP2, Endoplasmic Reticulum Aminopeptidase 2; FDR, false discovery rate; GWAS, genome-wide association study; HDAC7, Histone Deacetylase 7; HLA-DQB1, human leukocyte antigen DQ_Beta 1 Chain; KEAP1, Kelch Like ECH Associated Protein 1; NDFIP1, Nedd4 family interacting protein 1; NES, normalized enrichment score; PPP5C, Protein Phosphatase 5 Catalytic Subunit; RAVER1, Ribonucleoprotein, PTB-binding 1; RTEL-TNFR6B, Regulator Of Telomere Elongation Helicase 1- tumor necrosis factor receptor 6b; SBNO2, Strawberry Notch Homolog 2; SETD1A, SET domain containing 1A, histone lysine methyltransferase; SKAP2, Src Kinase Associated Phosphoprotein 2; STK11, Serine-Threonine Kinase 11.

To better understand how these gene expression patterns may emerge following biliary differentiation, we next analyzed whole exome sequencing data on 3 of our subjects with PSC (Supporting Table S1) for the gene set identified by the IPA and genome-wide association study analysis. The analysis identified 50 variants of unknown significance, including variants of many epigenetic regulators and transcription factors (e.g., HDAC7; BRF4; SWI/SNF related, matrix

associated, actin dependent regulator of chromatin, subfamily a, member 4 [SMARCA4]; SETD1A). Conceivably, the genetic variants noted in epigenetic regulators and transcription factors may be important for proper cholangiocyte differentiation. This may explain why the senescence phenotype is only unmasked after biliary differentiation. Overall, the data suggest that some PSC features (such as senescence) may have a genetic predisposition that can be

studied using this *in vitro* model system. These findings are similar to recent work published using an iPSC-derived hepatocyte system to study nonalcoholic steatohepatitis-related phenotypes.⁽⁸⁾

iDCs-DERIVED CHOLANGIOIDS FROM SUBJECTS WITH PSC HAVE INCREASED CELLULAR SENEESCENCE

Based on the gene expression profiling, the over-representation of senescence pathways was intriguing

because it has been shown that PSC is highly associated with senescence and the SASP.⁽⁴⁾ Given this, we hypothesized that the cells would indeed display features of cellular senescence and its consequences. Several studies have described the development of 3D cultures from cholangiocytes to model biliary diseases, such as Alagille's syndrome, polycystic liver disease, and cystic fibrosis.⁽⁹⁻¹²⁾ Previously, we generated epithelial organoids from 3D-cultured cholangiocytes (cholangioids) and were able to recapitulate features of senescence and SASP.⁽¹³⁾ Thus, to evaluate for senescence and SASP in our patient-derived samples,

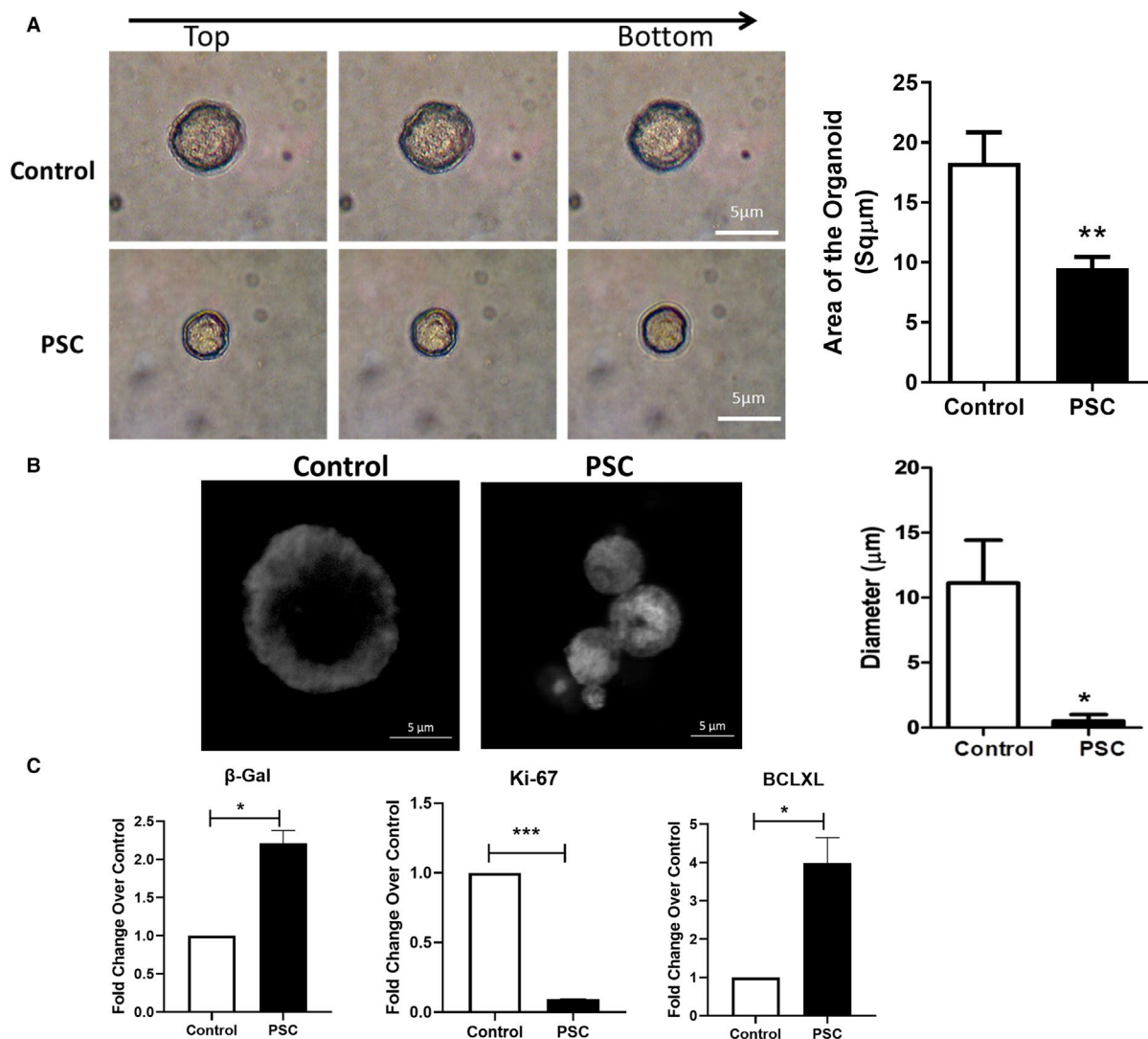


FIG. 5. Comparison of cholangioids from iPSC-derived iDCs. (A) Top to bottom view of cholangioids from healthy control and PSC iDCs from patient 3 (left), fold change on quantification of size of the cholangioids (right). (B) Image of cholangioids stained with membrane dye (left), quantification of the lumen diameter (right). (C) RT-PCR analysis for β -gal, Ki-67, and BCL-XL on cholangioids obtained from a healthy control and PSC patient 3; Data shown as Mean \pm SEM ** $P < 0.001$, * $P < 0.01$, *** $P < 0.0001$. Abbreviation: BCL-XL, B-cell lymphoma-extra large.

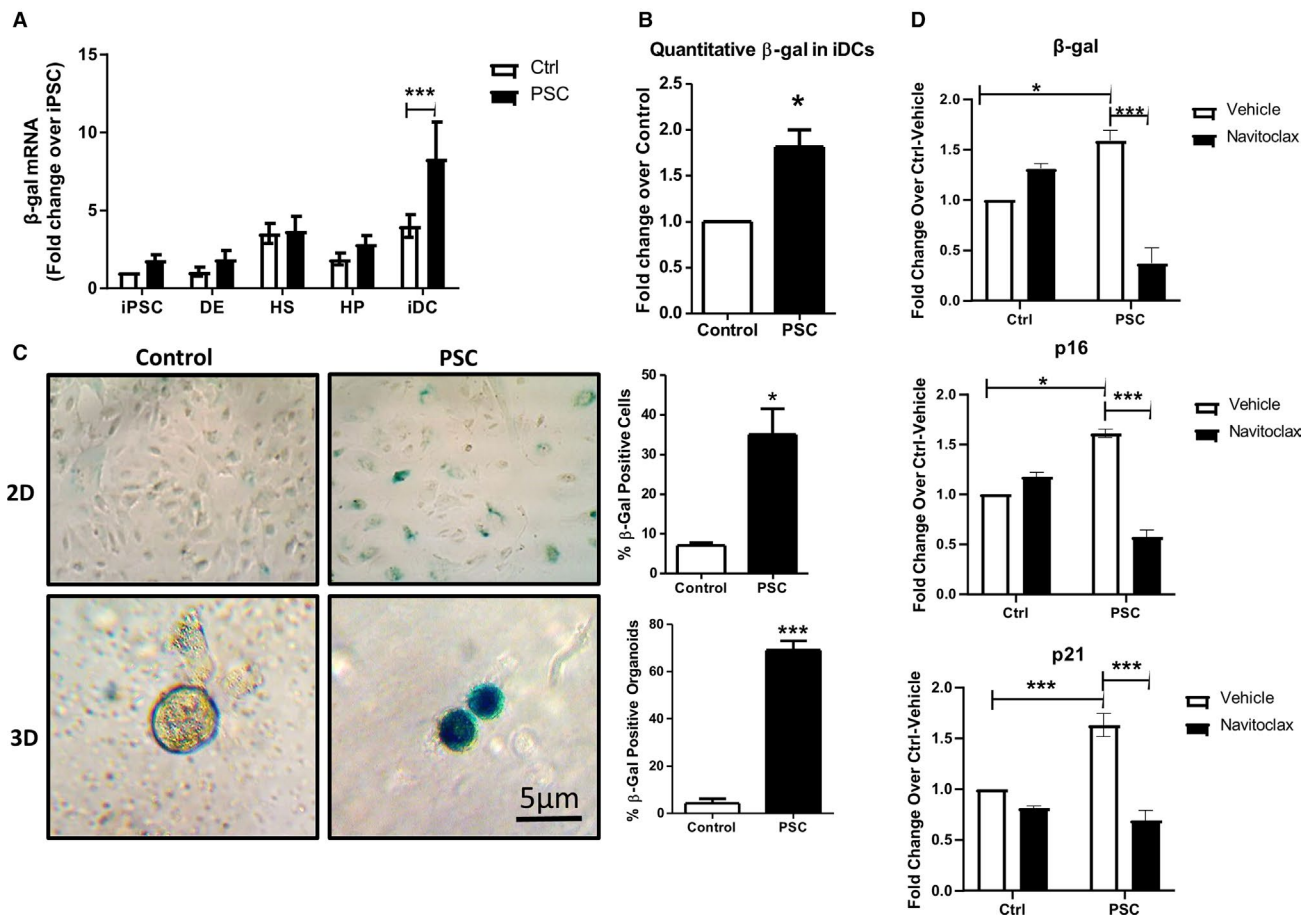


FIG. 6. Evaluation of senescence in iDCs. (A) RT-PCR analysis for β -gal expression in iPSC to iDC differentiation stages from a healthy control and PSC patient 3. (B) Quantitative β -gal analysis on iDCs from a healthy control and PSC patient 3. (C) β -gal staining on iDCs in 2D and 3D from a healthy control and PSC patient 3 (left); quantification showing percentage of β -gal-positive cells. (D) RT-PCR analysis for β -gal, p16, and p21 on iDCs from a healthy control and PSC patient 3 treated with navitoclax; Data shown as Mean \pm SEM *** P < 0.0001, * P < 0.01. Abbreviations: Ctrl, control; mRNA, messenger RNA.

we used the published protocol to generate epithelial organoids from both healthy control samples and PSC-derived iDCs. Consistent with the senescence phenotype, cholangioids from PSC-derived iDCs were significantly smaller in size compared to those from healthy controls (mean \pm SEM, $18.3 \pm 2.5 \mu\text{m}^2$ vs. $9.5 \pm 0.92 \mu\text{m}^2$; P < 0.005) (Fig. 5A). This phenotype persisted even when fewer cells were used for cholangioid formation (Supporting Fig. S9A). These data were consistent with our published observation that cholangioids from senescent cholangiocytes are uniformly smaller compared to the nonsenescent cells.⁽¹³⁾ Furthermore, when we stained these cholangioids with a membrane dye, we observed that the normal cholangioids had a lumen greater than 10 μm , which

was lacking in the PSC-derived cholangioids (Fig. 5B; Supporting Fig. S9B), also in concordance with our prior study. Next, we used RT-PCR to evaluate for gene expression changes in β -gal, a well-characterized marker of cellular senescence. We noted significant increases in β -gal expression in PSC-derived cholangioids compared to control samples (Fig. 5C). We also noted decreases in the proliferation marker Ki-67 and an increase in the apoptosis resistance gene B-cell lymphoma-extra large (BCL-XL). These data correlate with published findings of increased apoptosis resistance in senescent cholangiocytes⁽¹⁴⁾ We further evaluated the senescence phenotype at different stages of differentiation. Interestingly, the increase in β -gal expression was only present in the final stage of

differentiation, suggesting that the senescence phenotype is only unmasked following biliary differentiation (Fig. 6A). iDC senescence changes were further evaluated using a quantitative β -gal assay on the iDCs, and this analysis confirmed that PSC-derived iDCs have nearly 2-fold greater levels of senescence compared to controls (Fig. 6B). Immunohistochemical staining of the iDCs in both 2D and 3D culture confirmed an increase in positive β -gal staining in PSC samples compared to controls (Fig. 6C). No positive β -gal stain was observed in patient fibroblasts or iPSCs,

confirming that this phenotype is only recognized following biliary differentiation (Supporting Fig. S10). Lastly, we treated our control and PSC-derived iDCs with the senolytic agent navitoclax for 24 hours. RT-PCR analysis on the treated cells showed a reduction in senescence markers (β -gal, p16, and p21) with navitoclax treatment in PSC-iDCs (Fig. 6D). Taken together, these findings corroborate our RNA-seq analysis where senescence was overrepresented as one of the disease features present in the patient-derived iDCs. Furthermore, this senescence phenotype was

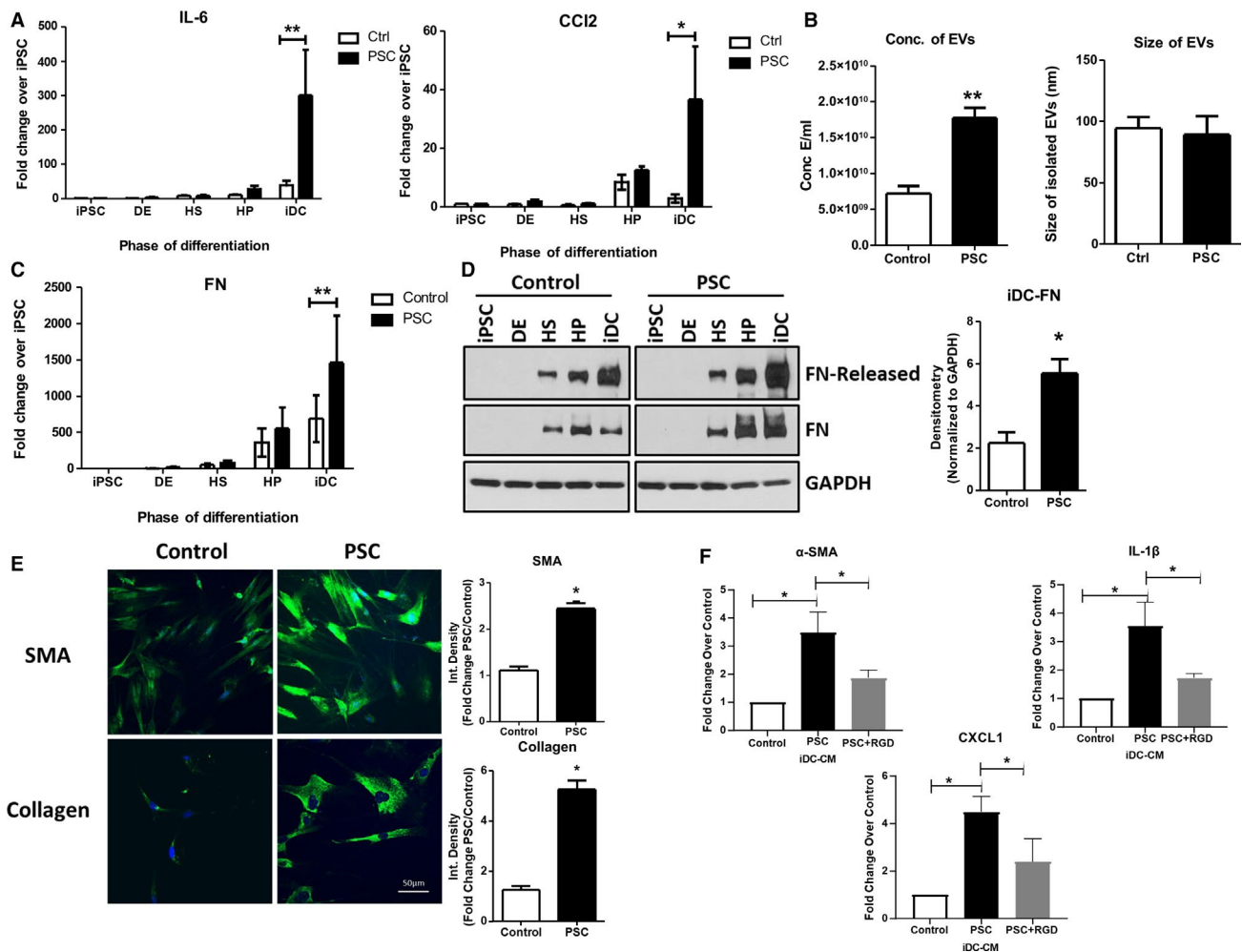


FIG. 7. Secretory features of iDCs. (A) RT-PCR analysis for IL-6 and CCL2 on iPSC to iDC differentiated cells from a healthy control and PSC patient 3. (B) Nanoparticle tracking analysis on EVs isolated from CM of iDCs of a healthy control and PSC patient 3. (C) RT-PCR analysis for FN on iPSC to iDC differentiated cells from a healthy control and PSC patient 3. (D) Western blot analysis for FN on iDCs and CM of iDCs (left), densitometry analysis on FN expression in iDCs normalized to GAPDH (right). (E) Immunofluorescence staining for α -SMA and collagen in HSCs incubated with CM of iDCs derived from healthy and PSC clones (left). Quantification of integrated density for α -SMA and collagen as fold change (right). (F) RT-PCR analysis for α -SMA, IL-1 β , and CXCL1 from HSCs treated with iDC-CM with or without RGD peptide; Bar graphs represent Mean \pm SEM. ** $P < 0.001$, * $P < 0.01$. Abbreviations: Ctrl, control; CXCL1, chemokine (C-X-C motif) ligand 1; GAPDH, glyceraldehyde 3-phosphate dehydrogenase; Int., integrated.

apparent only in the final stage of cholangiocyte differentiation, suggesting biliary specificity.

iDCs FROM SUBJECTS WITH PSC DISPLAY SASP AND ACTIVATE HSC

In order to evaluate whether iDCs derived from patients with PSC can provoke the SASP, we analyzed for expression of typical SASP-associated inflammatory cytokines IL-6 and C-C motif chemokine ligand 2 (CCL2). We noted significant increases in both IL-6 (mean \pm SEM, 10.3-fold \pm 3.7-fold; $P < 0.05$) and CCL2 (mean \pm SEM, 22-fold \pm 6.5-fold; $P < 0.05$) in iDCs derived from subjects with PSC. Consistent with the senescence data, the increased generation of SASP-associated markers (IL-6, CCL2) was only present in the iDC phase and not the earlier phases of differentiation (Fig. 7A). Also, consistent with the SASP, we detected an approximately 2.5-fold increase in the number of EVs released from PSC-derived samples (Fig. 7B). Because PSC is a fibrosing cholangiopathy and senescent cholangiocytes release paracrine activators of HSC, we evaluated the expression and release of fibronectin (FN). FN released from activated cholangiocytes is a canonical paracrine mediator of myofibroblast activation that subsequently leads to deposition of extracellular matrix during biliary fibrogenesis.⁽¹⁵⁾ RT-PCR analysis showed increased expression of FN as the differentiation proceeded. However, PSC-derived iDCs showed significantly increased FN expression compared to control iDCs (Fig. 7C). The increased expression was further confirmed by western blotting for FN during each phase of the differentiation process. Not only did we observe increased FN production in cell lysates from PSC-derived iDCs (mean \pm SEM, 4.12-fold \pm 1.13-fold; $P < 0.01$), we also noted a nearly 3-fold increase in the release of FN into the culture media (Fig. 7D). In order to evaluate whether cholangioids derived from subjects with PSC could more potently activate HSCs, we used CM experiments. To test the activating potential of CM from PSC-iDCs, we cultured primary human HSCs with CM derived from control iDCs or the media of iDCs derived from subjects with PSC. Immunofluorescence for typical markers of HSC activation (α -SMA and collagen) revealed increased HSC activation by CM derived from PSC-iDCs compared to that from control iDCs (Fig. 7E). Indeed, we found an increase in α -SMA (mean \pm SEM, 2.44-fold \pm 0.11-fold; $P < 0.0001$) and

collagen staining (mean \pm SEM, 5.26-fold \pm 0.34-fold; $P < 0.005$). We also performed RT-PCR analysis for the HSC activation marker SMA as well as inflammatory markers, including chemokine (C-X-C motif) ligand 1 (CXCL1) and IL-1 β (Fig. 7F). One common HSC activator in cholangiocyte media is FN, as we previously characterized.⁽¹⁵⁾ We therefore used the RGD peptide, which blocks FN binding to the integrin receptors on HSCs. RT-PCR analysis of the HSCs incubated with iDC-conditioned medium in the presence of RGD showed less activation (Fig. 7F). Overall, the secretory phenotype and the HSC activation potential revealed functional abnormalities of the patient-derived iDCs.

Discussion

The current study demonstrates that iPSC from patients with PSC differentiate efficiently to cholangiocytes and form epithelial organoids in 3D culture. Furthermore, PSC-derived cholangiocytes display disease-specific features, including PSC-related gene expression changes, luminal narrowing of organoids, cellular senescence, an inflammatory and fibrogenic SASP, and an increased ability to activate HSCs. The inflammatory profile observed in our system corroborates with a recent study on organoids derived from bile of patients with PSC.⁽¹⁶⁾ Our work suggests that PSC cholangiocytes are intrinsically predisposed to cellular senescence and its consequences, presumably through genetic and/or epigenetic mechanisms. The significance of these observations lies in the concept that biliary differentiation itself unmasks a senescence phenotype in PSC-derived cholangiocytes that is not present in the skin fibroblasts or in the reprogrammed iPSC. This approach provides a novel source of cells for modeling certain cholangiocyte-intrinsic aspects of PSC, such as senescence, and may serve as a platform for testing senolytic therapies.

The past decade has seen remarkable advances in stem cell technology, including simpler and more accessible methods of reprogramming somatic cells to pluripotency.⁽¹⁷⁾ Furthermore, a variety of differentiation protocols have emerged that allows the generation of multiple adult cell types for disease modeling and pharmacologic testing. With respect to the liver, several well-characterized protocols now exist for generating hepatocyte-like cells and cholangiocytes.^(5,9,10,18,19)

While these technologies are most obviously suited to study purely genetic disorders with known mutations (e.g., polycystic liver disease, cystic fibrosis-related cholangiopathy), there is also an opportunity to study cell-intrinsic features of complex disorders that may have genetic and epigenetic factors.⁽²⁰⁾ For these reasons, we have populated a robust biorepository of skin fibroblasts and iPSCs from subjects with a variety of hepatocellular and cholestatic liver diseases for future studies (Table 1).

In this study, we initially evaluated the quality of iPSCs derived from healthy subjects and those with PSC. We report that skin fibroblasts from subjects with PSC can be reprogrammed with similar efficiency as those derived from healthy subjects, based on expression of pluripotency markers, flow cytometry, karyotype analysis, and trilineage differentiation. We also found that PSC-derived iPSCs differentiate efficiently to iPSC-derived cholangiocytes, based on their temporal acquisition of the biliary-specific cytokeratins CK7 and CK19. We used RNA-seq to compare the transcriptome of iDCs derived from healthy subjects or subjects with PSC as well as three cholangiocyte cell lines derived from the isolated cholangiocytes of subjects with PSC. We found that PSC-derived iDCs share transcriptome differences with cells derived from patients with PSC, particularly in pathways related to cellular senescence. These findings suggest alterations present in skin fibroblasts from subjects with PSC that then have functional consequences following reprogramming and differentiation. Indeed, whole exome sequencing identified several genetic variants in the PSC samples that correspond with epigenetic regulators and transcription factors. While cellular senescence has been observed in PSC liver and is increasingly implicated in the pathophysiology of the disease, these are the first data to suggest that a predisposition to cholangiocyte senescence may be cell intrinsic, genetically encoded, and/or epigenetically activated during biliary differentiation. While such mechanisms are likely to be highly complex, it is tempting to speculate that mutations in certain epigenetic regulators may lead to an altered transcriptional profile in a temporal context-dependent manner. It appears that these changes only become apparent as liver progenitor cells reach their terminal phase of cholangiocyte development. Further studies will be needed to confirm and clarify these ideas, but our study suggests that individualized disease modeling with iDCs may be an important tool in this regard.

Having identified changes in senescence pathways, we then sought to further evaluate morphologic and functional characteristics of the iDCs in 3D culture. Our prior studies have shown that cholangiocyte epithelial organoids (cholangioids) derived from cellular models of PSC result in cholangioids that are smaller in size and lack a central lumen.⁽¹³⁾ Similarly, the iDC-derived organoids from subjects with PSC are also approximately half the size of those derived from healthy subjects and they display near complete obliteration of the central luminal space. We confirmed that PSC-derived iDCs display cellular senescence in both 2D- and 3D-culture conditions. Interestingly, the differences in senescence are not present in the skin fibroblasts, the iPSC cells, or in the intermediate phases of differentiation (DE, HS, and HP). In line with this, the PSC-derived iDCs take on a secretory profile consistent with the SASP, secreting large amounts of IL-6, CCL2, EVs, and FN into the culture media. Again, this phenotype is only unmasked in the final biliary phase of differentiation and is not present in the earlier phases. Predictably, the CM from these highly secretory cholangiocytes has the ability to more potently activate HSCs through paracrine mechanisms of epithelial–mesenchymal crosstalk, consistent with previous observations of the cholangiocyte secretome activating HSCs.^(15,21)

Our study, while intriguing, has a variety of important limitations to be considered. First, while we have recruited a large number of subjects for skin biopsy, the time- and resource-intensive nature of the iPSC and organoid technologies leads to smaller numbers ultimately being analyzed. Especially given the considerable heterogeneity of PSC phenotypes within and between patients, important features could have been either overrepresented or overlooked. We chose to study patients with advanced PSC who were undergoing transplantation because it allowed us to simultaneously obtain skin fibroblasts from the transplant recipients and the corresponding living donors. The living donors are thoroughly prescreened to ensure no occult liver disease, making them excellent healthy control subjects. Analyzing reprogrammed iPSC lines derived from patients with earlier stages of PSC as well as other cholestatic diseases can be important goals for future studies. Further studies will also be needed to determine whether the senescence features are also found in primary biliary cirrhosis and other idiopathic cholestatic diseases. Multiple methods have

been developed for cholangiocyte differentiation from iPSCs^(9,10) and for generation of cholangiocyte organoids.⁽²⁰⁾ While the various techniques are all broadly similar in principle, different protocols could yield different results. Furthermore, while it seems that iDCs have a more mature phenotype in general than iPSC-derived hepatocyte-like cells,⁽¹⁷⁾ it is possible that iDCs lack a fully mature cholangiocyte phenotype. Lastly, the genetic and epigenetic underpinnings of the changes we observe in gene expression, cellular senescence, and HSC activation will require further investigation.

In summary, we report differentiation and characterization of cholangiocytes from skin fibroblasts of patients with PSC and generation of epithelial organoids. The results reveal differentiation-dependent differences in gene expression, organoid morphology, cellular senescence, SASP, and HSC activation potential. The results suggest that PSC cholangiocytes are predisposed to cellular senescence and its consequences and highlight the utility of iPSCs and organoid systems for modeling various aspects of complex genetic cholangiopathies.

Acknowledgment: We acknowledge technical assistance from Karen Krucker, coordinator support from Lindsay Mulvihill, and secretarial services from Deb Hintz.

REFERENCES

- 1) Lazaridis KN, LaRusso NF. Primary sclerosing cholangitis. *N Engl J Med* 2016;375:2501-2502.
- 2) Meng L, Quezada M, Levine P, Han Y, McDaniel K, Zhou T, et al. Functional role of cellular senescence in biliary injury. *Am J Pathol* 2015;185:602-609.
- 3) Tabibian JH, Trussoni CE, O'Hara SP, Splinter PL, Heimbach JK, LaRusso NF. Characterization of cultured cholangiocytes isolated from livers of patients with primary sclerosing cholangitis. *Lab Invest* 2014;94:1126-1133.
- 4) Tabibian JH, O'Hara SP, Splinter PL, Trussoni CE, LaRusso NF. Cholangiocyte senescence by way of N-ras activation is a characteristic of primary sclerosing cholangitis. *Hepatology* 2014;59:2263-2275.
- 5) **De Assuncao TM, Sun Y, Jalan-Sakrikar N, Drinane MC, Huang BQ, Li Y, et al.** Development and characterization of human-induced pluripotent stem cell-derived cholangiocytes. *Lab Invest* 2015;95:684-696. Erratum in: *Lab Invest* 2015;95:1218.
- 6) **Yaqoob U, Luo F, Greuter T, Jalan Sakrikar N, Schrawat TS, Lu J, et al.** GIPC-regulated IGFBP-3 promotes HSC migration in vitro and portal hypertension in vivo through a β 1-integrin pathway. *Cell Mol Gastroenterol Hepatol* 2020;10:545-559.
- 7) **Ji S-G, Juran BD, Mucha S, Folseraas T, Jostins L, Melum E, et al.;** UK-PSC Consortium; International IBD Genetics Consortium; International PSC Study Group. Genome-wide association study of primary sclerosing cholangitis identifies new risk loci and quantifies the genetic relationship with inflammatory bowel disease. *Nat Genet* 2017;49:269-273.

- 8) Duwaerts CC, Le Guillou D, Her CL, Phillips NJ, Willenbring H, Mattis AN, et al. Induced pluripotent stem cell-derived hepatocytes from patients with nonalcoholic fatty liver disease display a disease-specific gene expression profile. *Gastroenterology* 2021;160:2591-2594.e6.
- 9) Ogawa M, Ogawa S, Bear CE, Ahmadi S, Chin S, Li B, et al. Directed differentiation of cholangiocytes from human pluripotent stem cells. *Nat Biotechnol* 2015;33:853-861.
- 10) Sampaziotis F, de Brito MC, Madrigal P, Bertero A, Saeb-Parsy K, Soares FAC, et al. Cholangiocytes derived from human induced pluripotent stem cells for disease modeling and drug validation. *Nat Biotechnol* 2015;33:845-852.
- 11) Spirli C, Mariotti V, Villani A, Fabris L, Fiorotto R, Strazzabosco M. Adenylyl cyclase 5 links changes in calcium homeostasis to cAMP-dependent cyst growth in polycystic liver disease. *J Hepatol* 2017;66:571-580.
- 12) Waisbourd-Zinman O, Koh H, Tsai S, Lavrut P-M, Dang C, Zhao X, et al. The toxin biliatresone causes mouse extrahepatic cholangiocyte damage and fibrosis through decreased glutathione and SOX17. *Hepatology* 2016;64:880-893.
- 13) Loarca L, De Assuncao TM, Jalan-Sakrikar N, Bronk S, Krishnan A, Huang B, et al. Development and characterization of cholangioids from normal and diseased human cholangiocytes as an in vitro model to study primary sclerosing cholangitis. *Lab Invest* 2017;97:1385-1396.
- 14) O'Hara SP, Splinter PL, Trussoni CE, Guicciardi ME, Splinter NP, Al Suraih MS, et al. The transcription factor ETS1 promotes apoptosis resistance of senescent cholangiocytes by epigenetically up-regulating the apoptosis suppressor BCL2L1. *J Biol Chem* 2019;294:18698-18713.
- 15) Jalan-Sakrikar N, De Assuncao TM, Shi G, Aseem SO, Chi C, Shah VH, et al. Proteasomal degradation of enhancer of zeste homologue 2 in cholangiocytes promotes biliary fibrosis. *Hepatology* 2019;70:1674-1689.
- 16) Soroka CJ, Assis DN, Alrabadi LS, Roberts S, Cusack L, Jaffe AB, et al. Bile-derived organoids from patients with primary sclerosing cholangitis recapitulate their inflammatory immune profile. *Hepatology* 2019;70:871-882.
- 17) Ellis J, Bhatia M. iPSC technology: platform for drug discovery. *Point. Clin Pharmacol Ther* 2011;89:639-641.
- 18) **Si-Tayeb K, Noto FK, Nagaoka M, Li J, Battle MA, Duris C, et al.** Highly efficient generation of human hepatocyte-like cells from induced pluripotent stem cells. *Hepatology* 2010;51:297-305. Erratum in: *Hepatology* 2010;51:1094.
- 19) Song Z, Cai J, Liu Y, Zhao D, Yong J, Duo S, et al. Efficient generation of hepatocyte-like cells from human induced pluripotent stem cells. *Cell Res* 2009;19:1233-1242.
- 20) Fiorotto R, Amenduni M, Mariotti V, Fabris L, Spirli C, Strazzabosco M. Liver diseases in the dish: iPSC and organoids as a new approach to modeling liver diseases. *Biochim Biophys Acta Mol Basis Dis* 2019;1865:920-928.
- 21) Aseem SO, Jalan-Sakrikar N, Chi C, Navarro-Corcuera A, De Assuncao TM, Hamdan FH, et al. Epigenomic evaluation of cholangiocyte transforming growth factor- β signaling identifies a selective role for histone 3 lysine 9 acetylation in biliary fibrosis. *Gastroenterology* 2021;160:889-905.e10.

Author names in bold designate shared co-first authorship

Supporting Information

Additional Supporting Information may be found at onlinelibrary.wiley.com/doi/10.1002/hep4.1809/supinfo.